Advanced Synthesis & Catalysis

ADVANCED SYNTHESIS & CATALYSIS
advsynthcatal.com

RESEARCH ARTICLE OPEN ACCESS

Asymmetric Synthesis of Atropisomeric Amines via Transaminase-Catalyzed Dynamic Kinetic Resolution

Juan M. Coto-Cid[1] | Patricia Rodríguez-Salamanca[2] | Christian M. Heckmann[3] | Caroline E. Paul[3] | Joaquín López-Serrano[4] | Rosario Fernández[1] | José M. Lassaletta[2] | Valentín Hornillos[1] | Gonzalo de Gonzalo[1]

[1]Department of Organic Chemistry, University of Seville, Seville, Spain | [2]Instituto de Investigaciones Químicas (CSIC-US) and Centro de Innovación en Química, Avanzada (ORFEO–CINQA), Seville, Spain | [3]Department of Biotechnology, Delft University of Technology, Delft, The Netherlands | [4]Departamento de Química Inorgánica and Centro de Innovación en Química Avanzada (ORFEO-CINQA), Instituto de Investigaciones Químicas (CSIC-US), Sevilla, Spain

Correspondence: José M. Lassaletta (jmlassa@iiq.csic.es) | Valentín Hornillos (vhornillos@us.es) | Gonzalo de Gonzalo (gdegonzalo@us.es)

Received: 22 July 2025 | **Revised:** 7 November 2025 | **Accepted:** 15 November 2025

Keywords: atroposelective synthesis | dynamic kinetic resolutions | selective aminations | transaminases

ABSTRACT

Atropisomeric heterobiaryl primary amines are of significant interest in both organic and pharmaceutical chemistry. A series of transaminases have been employed to synthesize these valuable compounds with high yields (up to 98% conversion) and excellent enantioselectivities (up to ≥99% *ee*) via dynamic kinetic resolution of the corresponding heterobiaryl aldehydes. This process features a Lewis acid–base interaction strategy to facilitate labilization of the stereogenic axis.

1 | Introduction

Axially chiral heterobiaryl amines are an important class of compounds with significant interest in organic synthesis due to their presence in natural products [1–3], pharmaceuticals [2, 4], and chiral ligands [5–12]. These compounds exhibit diverse biological activities and represent a widely prevalent scaffold in drug discovery, particularly in the development of kinase inhibitors, anticancer agents, and central nervous system drugs. In addition, heterobiaryl amines serve as key intermediates in the synthesis of functional materials, including organic light-emitting diodes and organic semiconductors [13–15]. A particularly important family within this class of compounds is that of axially chiral biaryl benzylamines, which are prevalent in a wide variety of bioactive molecules, such as allocolchicine and vancomycin [16, 17], and play a key role as alkylamine-derived chiral catalysts [18–20] (Figure 1).

The stereoselective synthesis of these compounds remains challenging, as the presence of an aliphatic amino group can interfere with catalytic cycles, thereby requiring extended synthetic sequences to overcome this limitation. In this regard, traditional methods for the synthesis of axially chiral benzyl amines have relied on the use of chiral substrates, such as benzyl halides, amides, and azides [21–23]. The swift advancement of transition metal- and organocatalyzed atroposelective methodologies has further enabled the development of more efficient and economically viable strategies for synthesizing these compounds [6, 24–29].

Recently, the Akiyama group identified biaryl hemiaminals as effective intermediates for dynamic kinetic resolution (DKR), owing to their facile in situ formation and ring opening. The resulting imine species can undergo asymmetric transfer hydrogenation (ATH), leading to axially chiral biaryl benzylamines with high enantiomeric excess [30]. This racemization-based approach was later integrated with hydrogen-borrowing catalysis to enable a redox-neutral amination of biaryl substrates [31]. We have also developed a strategy to synthesize axially chiral benzylaryldiamines, taking advantage of the formation of related bridged biaryl aminals to facilitate racemization. The fast equilibrium with the open-chain amino-imino tautomer enabled a DKR via Ru-catalyzed ATH, affording BINAM analogs in high

Juan M. Coto-Cid and Patricia Rodríguez-Salamanca contributed equally to this work.

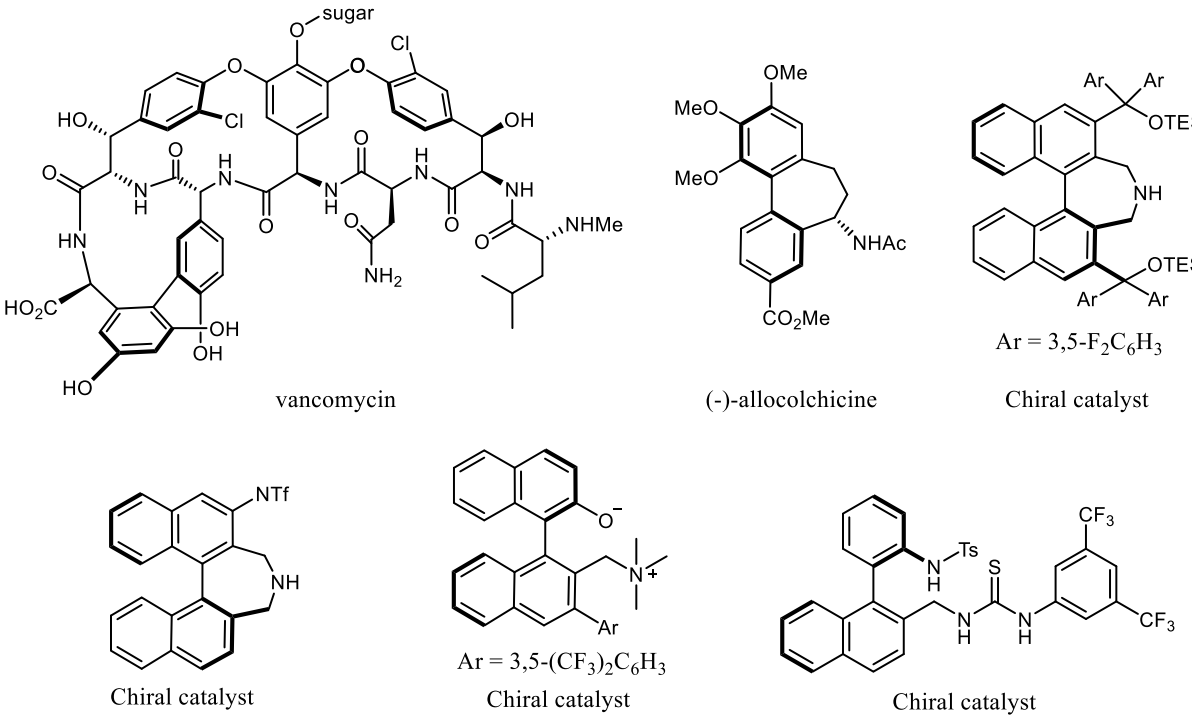

FIGURE 1 | Selected examples of natural products and catalyst containing axially chiral benzylamines.

enantioselectivities. More recently, a highly enantioselective Pictet–Spengler reaction catalyzed by chiral phosphoric acids was reported for synthesizing axially chiral tetrahydroisoquinolines [32].

Biocatalysis, which offers the advantage of proceeding under mild conditions while avoiding the use of heavy metals and oxidants and generating minimal byproducts, represents an excellent solution for the synthesis of these compounds [33–35]. However, biocatalytic methods for the synthesis of (hetero)biaryl benzylamine atropisomers remain limited. Early efforts using lipase-mediated kinetic resolution of racemic biaryl benzylamines faced significant challenges, including low yields (below 50%) and poor enantiomeric resolution [36]. Very recently, the desymmetrization of a set of biaryl dialdehydes using various amine donors, generating the corresponding chiral amines in the presence of different engineered imine reductases (IREDs) with high optical purities and good yields [37, 38].

The biocatalytic atroposelective synthesis of biaryl amines has also been accomplished through DKR of biaryl aldehydes with various amines [39]. The process involves an aza-acetal bridge-facilitated racemization of the initially formed racemic imine, followed by stereoselective reduction catalyzed by IREDs, yielding the targeted compounds with up to 99% enantiomeric excess and 99% conversion. IREDs have also been employed in the DKR of heterobiaryl and heterobiaryl *N*-oxide aldehydes, employing a racemization mechanism that involves the formation of cyclic transition states via interactions between the Lewis basic *N*-oxide and the weakly acidic carbonyl group. This approach enables the efficient synthesis of corresponding heterobiaryl secondary amines with excellent enantioselectivities in the presence of benzylamine [40].

Aminotransferases or transaminases (ATAs) are pyridoxal 5′-phosphate (PLP)-dependent enzymes that catalyze the transfer of an amino group from an amino donor to a keto acceptor molecule, offering a promising biocatalytic alternative for amine synthesis [41, 42]. ATAs are robust, engineerable enzymes featuring high enantioselectivities and a broad substrate scope, which makes them particularly attractive for green chemistry applications. Recent advances in protein engineering and directed evolution have further expanded their substrate scope and enhanced catalytic efficiency, enabling the synthesis of complex molecules containing amino groups in high yields and selectivities [43, 44]. For these reasons, ATAs are one of the most applied and scaled-up enzyme classes in industry [45].

Our group has demonstrated that relatively weak Lewis acid–base interactions (LABIs) between strategically positioned functionalities within (hetero)biaryl systems significantly reduce the rotational barrier, thereby facilitating racemization in sterically hindered substrates and enabling a DKR process [46–50]. With this aim, we have developed transformations aimed at disrupting these Lewis pair interactions, leading to configurationally stable and enantioenriched products. In this context, biocatalysis has proven to be an excellent approach for the preparation of optically active heterobiaryl alcohols and esters, achieving high yields and optical purities using alcohol dehydrogenases (Scheme 1A,C) [51, 52] and lipases (Scheme 1D) [53]. Herein, we describe the implementation of the LABI-based strategy for the synthesis of heterobiaryl amines, including *N*-arylindole diamines and 2-(quinolin-8-yl)benzyl amines via transaminase-mediated DKR (Scheme 1B,E).

2 | Results and Discussion

Initial screening experiments were conducted to optimize the biotransformation of the heterobiaryl indole aldehyde **1a** (5.0 mM), using a set of commercially available transaminases (Codexis ATAs Screening Kit). As shown in Table 1, ten ATAs

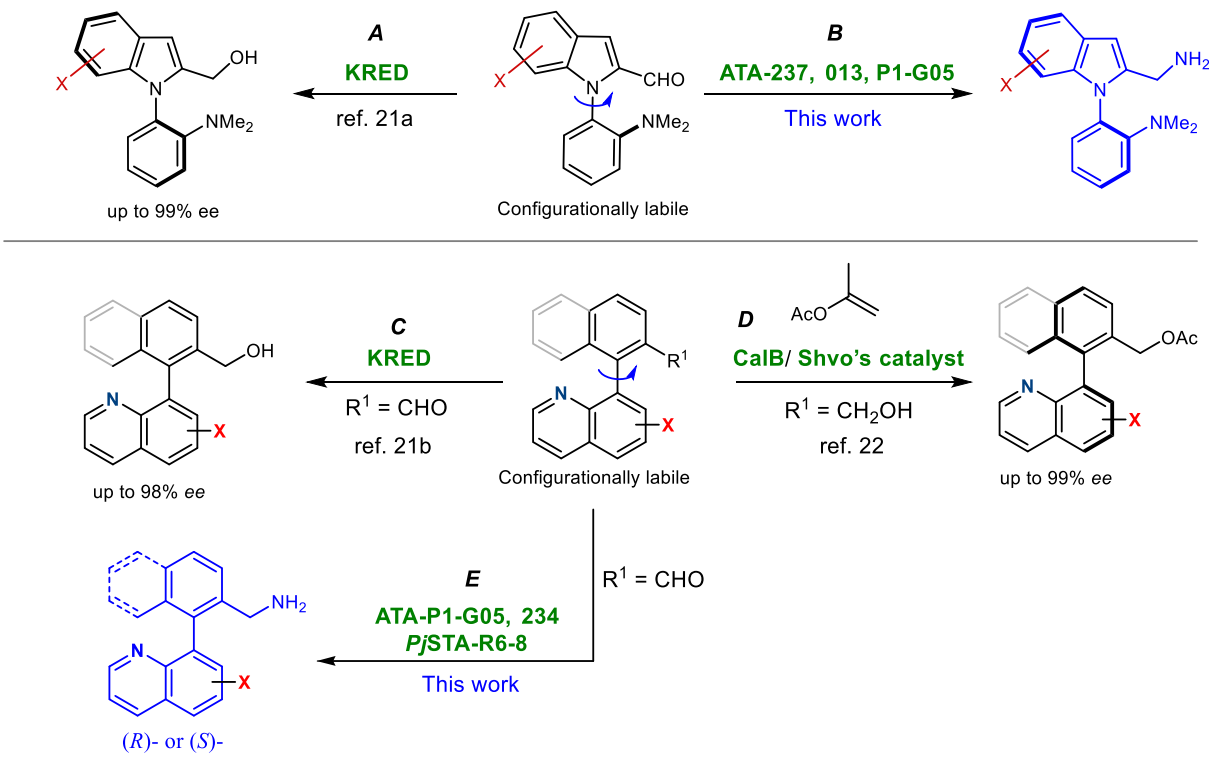

SCHEME 1 | Biocatalytic atroposelective DKR strategies based on LABIs as a racemization strategy. (A,C) DKRs of heterobiaryl alcohols catalyzed by ADHs; (B,E) Synthesis of N-arylindiole diamines and 2-(quinolin-8-yl)benzyl amines via transaminase-mediated DKR (this work); (D) Chemoenzymatic DKR of racemic heterobiaryl alcohols employing CalB and Shvo's Catalyst.

TABLE 1 | DKR of heterobiaryl aldehyde (±)-**1a** employing commercially available ATAs. Substrate (5 mM) was dissolved in an ethanolamine buffer 0.1 M pH 7.5 with 10% v/v DMSO containing PLP (1.0 mM), $^{i}PrNH_2$ (1.0 M), and the corresponding ATA (10 mg).

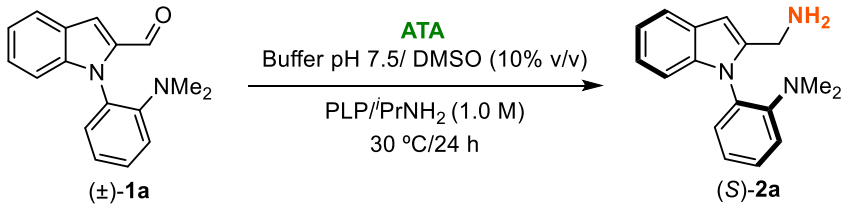

Entry	TA	[%]-2a[a]	*ee* (*S*)-2a, %[b]
1	ATA-013	97	96
2	ATA-025	95	93
3	ATA-217	97	7
4	ATA-234	97	29
5	ATA-237	97	73
6	ATA-238	97	12
7	ATA-303	30	≤3
8	ATA-412	13	≤3
9	ATA-415	97	97
10	ATA-P1-G05	71	79

Abbreviations: GC/MS, gas chromatography/mass spectrometry; HPLC, high performance liquid chromatography.
[a]Determined by Gas chromatography/Mass spectrometry.
[b]Determined by HPLC after acetylation of the resulting amine **2a**.

successfully catalyzed the formation of amine **2a**, consistently yielding the *S*-configured diamine atropisomer. While ATA-303 and ATA-412 displayed low activity and lacked enantioselectivity (entries 7 and 8, respectively), the remaining transaminases produced appreciable amounts of the target amine. ATAs 217, 234, and 238 yielded (*S*)-**2a** with low optical

purities (entries 3, 4, and 6), whereas ATA-237 and ATA-P1-G05 showed improved enantioselectivity, affording the corresponding chiral amine with 73% *ee* (entry 5) and 79% ee (entry 10), respectively. The best results were obtained using ATA-013, ATA-025, and ATA-415, which enabled the biocatalytic reductive amination with near-complete conversions and excellent optical purities, exceeding 93% *ee* (entries 1, 2, and 9). Notably, ATA-415 delivered (*S*)-**2a** with 97% conversion and 97% *ee*.

The influence of the substrate concentration of **1a** on the activity and selectivity of ATA-013 was evaluated. To enable comparison across reactions conducted at different times, the space time yield was defined as the millimoles of **1a** consumed per liter per hour. Bioconversion of aldehyde to amine (*S*)-**2a** increased with substrate concentrations above 5.0 mM, reaching a maximum reaction rate of 44.2 mmol L^{-1} h^{-1} at 40 mM. The reaction rate decreased at higher concentration, yielding 28.3 mmol L^{-1} h^{-1} at 80 mM. Nonetheless, this value remains higher than the rate observed at 5 mM (18.8 mmol L^{-1} h^{-1}). Across all substrate concentrations studied, no effect on the amine selectivity was observed, with (*S*)-**2a** consistently obtained in excellent optical purities.

Using the most efficient ATAs, we further explored the scope of this biocatalytic atroposelective amination strategy by using a series of 2-formylindoles **1b–h**, bearing different substituents on the indole ring (Scheme 2). Excellent results were obtained in the amination of fluorinated derivatives, including 4-fluoro (**1d**) and 6-fluoro (**1e**), as well as 6-methyl (**1g**) and 4-methoxy (**1h**) substituted aldehydes, all exhibiting optical purities higher than 90%. For instance, (*S*)-**2e** was obtained with 98% conversion and 91% enantiomeric excess after 24 h using ATA-013 as the catalyst, while enantiopure (*S*)-**2g** was obtained with complete conversion when the same enzyme was used. In contrast, indoles bearing 5- and 6-chlorine or 5-methyl substituents exhibited moderate enantioselectivities, with enantiomeric excess values ranging from 52% to 77%. Notably, no amination reaction was observed for heterobiaryl aldehydes featuring a methyl substituent at the 3-position of the indole ring or a trifluoromethyl group on the phenyl moiety.

Subsequently, we investigated the biocatalytic reductive amination of additional configurationally labile heterobiaryl aldehydes under DKR conditions. Specifically, quinoline-based aldehydes bearing naphthyl or tolyl substituents were evaluated as substrates for the ATAs. Overall, these compounds exhibited lower reactivity compared to the indole-derived aldehydes. The reaction of 1-(quinolin-8-yl)-2-naphthaldehyde (**1i**) with most of the biocatalysts tested failed to produce the desired amine **2i** (Table S4). The highest yield was observed using ATA-P1-G05 which afforded (*R*)-**2i** in 26% yield with excellent enantioselectivity (97% *ee*, entry 1, Table 2). Extending the reaction time to 72 h resulted in an increased conversion of 65% conversion while maintaining the same optical purity (entry 8). ATA-217 also afforded (*R*)-**2i** with good optical purities (around 80%), albeit with moderate conversion (entry 3). In contrast, ATA-234 yielded slightly lower conversion and enantiomeric excesses. ATAs 237 and 238 were able to catalyze the formation of the opposite atropisomer [(*S*)-**2i**], but with low conversions and moderate optical purities, as shown in entries 5 and 6. In view of these results, the reductive amination was also explored using ATA-117 from *Arthrobacter* sp. and *Pj*STA-R6-830 from *Pseudomonas jessenii*, both previously reported for their efficacy in synthesizing other *N*-heterocycles [54, 55]. While ATA-117 exhibited no activity

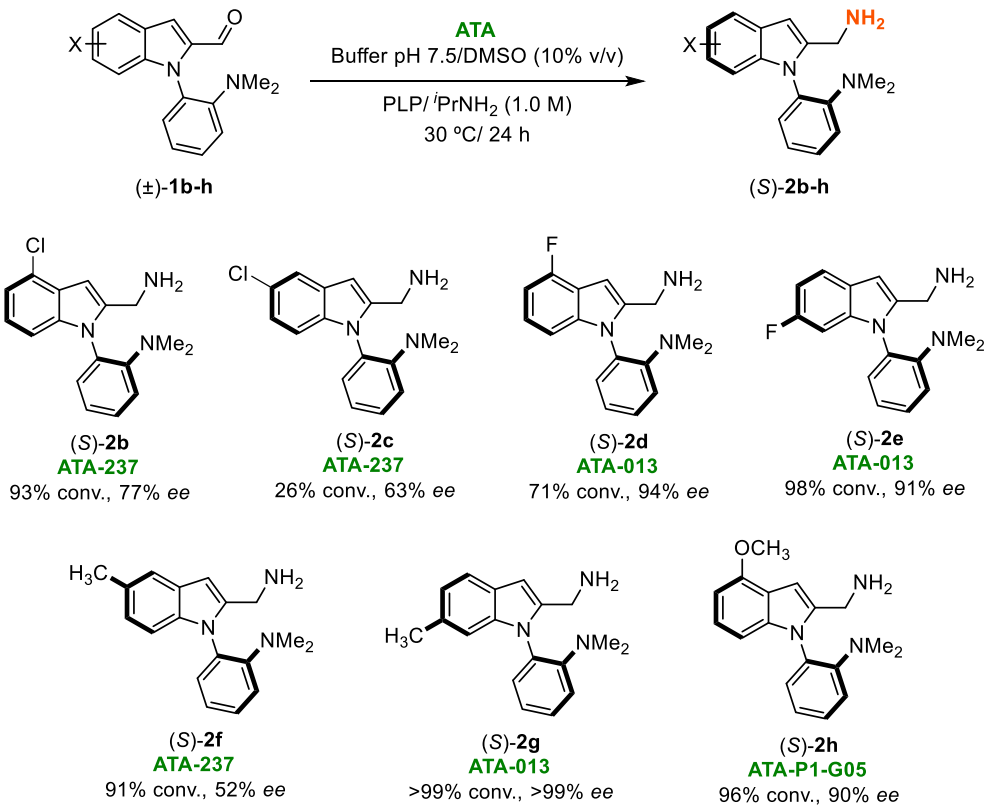

SCHEME 2 | Synthesis of heterobiaryl amines (*S*)-**2b–h** through DKR employing ATAs. Substrate (5 mM) was dissolved in an ethanolamine buffer 0.1 M pH 7.5 with 10% v/v DMSO containing PLP (1.0 mM), $^{i}PrNH_2$ (1.0 M), and the corresponding ATA (10 mg).

TABLE 2 | DKR of heterobiaryl aldehydes (±)-**1i–m** employing commercially available ATAs. Aldehyde (5 mM) was dissolved in an ethanolamine buffer 0.1 M pH 7.5 with 10% v/v DMSO containing PLP (1.0 mM), $^{i}PrNH_2$ (1.0 M), and the corresponding ATA (10 mg).

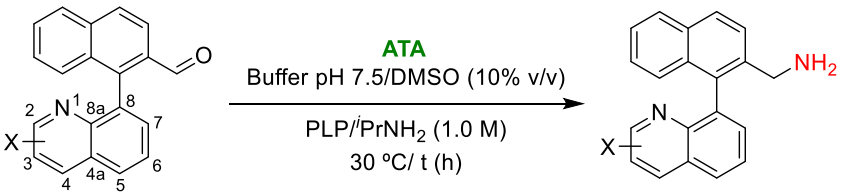

(±)-**1i-k**

(*R*)- or (*S*)-**2i-k**

1i: X: H
1j: X: 5-Cl
1k: X: 6-CF_3
1l: X: 4-CH_3
1m: X: 6-CH_3

Entry	X	ATA	*t*, h	[%]-2i–k[a]	*ee* (*S*)-2i–k, %[a]	Config.
1	H	ATA-P1-G05	24	26	97	*R*
2	H	ATA-P1-B04	24	10	82	*S*
3	H	ATA-217	24	29	82	*R*
4	H	ATA-234	24	21	81	*R*
5	H	ATA-237	24	15	52	*S*
6	H	ATA-238	24	18	37	*S*
7	H	*Pj*STA-R6-8	48	45	85	*S*
8	H	ATA-P1-G05	72	65	97	*R*
9	H	*Pj*STA-R6-8	72	66	86	*S*
10	5-Cl	ATA-234	24	10	73	*R*
11	6-CF_3	ATA-234	24	28	45	*R*
12	4-CF_3	*Pj*STA-R6-8	24	31	≥99	*S*
13	4-CH_3	ATA-234	24	51	83	*R*
14	4-CH_3	*Pj*STA-R6-8	24	30	≥99	*S*
15	6-CH_3	ATA-234	24	85	79	*R*

[a]Measured by HPLC after acetylation of the resulting amines.

(Table S4), the amination reaction of racemic **1i** catalyzed by *Pj*STA-R6-8 yielded the opposite atropisomer to ATA-P1-G05, affording (*S*)-**2i** with 45% conversion and 86% *ee* after 48 h (entry 7), whereas performing the reaction for 72 h led to an increase of the conversion (65%, entry 9), while the optical purity is maintained. Therefore, through appropriate biocatalyst selection, both atropisomers of amine **2i** can be obtained with good optical purities.

To gain insight into the origin of the enantioselectivity, we carried out docking studies on *Pj*STA-R6-8. We docked the quinonoid intermediate of both (*R*)- and (*S*)-**1i** into the active site using YASARA, observing steric clashes and lower docking scores for the (*R*)-enantiomer compared to the (*S*)-enantiomer (Figure 2). Thus, it appears that the origin of the selectivity is due to steric interaction in the active site. It should be noted that the docking algorithm treated the dihedral angle of the chiral axis as completely rigid, docking poses should be viewed with the appropriate level of caution. However, this rigidity assumption is not unreasonable, as the rotation around the chiral axis is most likely restricted within the enzyme active site.

Other heterobiaryl aldehydes bearing substituents on the quinoline ring, namely, **1j** (X: 5-Cl) and **1k** (X: 6-CH_3), were also evaluated. The use of ATA-234 afforded exclusively the corresponding (*R*)-amines, with amine **2j** being obtained in moderate conversion and 73% ee (entry 10). In contrast, the 6-trifluoromethyl derivative was converted into enantiopure (*S*)-**2k** in 31% conversion using PjSTA-R6-8, whereas the (*R*)-amine was obtained with a similar conversion but a significantly lower enantiomeric excess (entry 11). Furthermore, aldehyde **1m** gave (*S*)-**2m** in 75% conversion and 80% *ee* (entry 15). For the aldehyde bearing a methyl substituent at the 4-position, both amine enantiomers could be obtained depending on the biocatalyst employed. PjSTA-R6-8 catalyzed the transamination with 30% conversion, providing enantiopure (*S*)-**2l** (entry 13), whereas ATA-234 afforded (*R*)-**2l** in 50% conversion and 83% *ee* (entry 14).

To improve the performance of P1-G05 and *Pj*STA-R6-8 in the synthesis of (*R*)- and (*S*)-**2i**, respectively, the effect of the reaction cosolvent was investigated. Biocatalytic aminations were conducted using 10% v/v DMSO as a cosolvent to enhance substrate

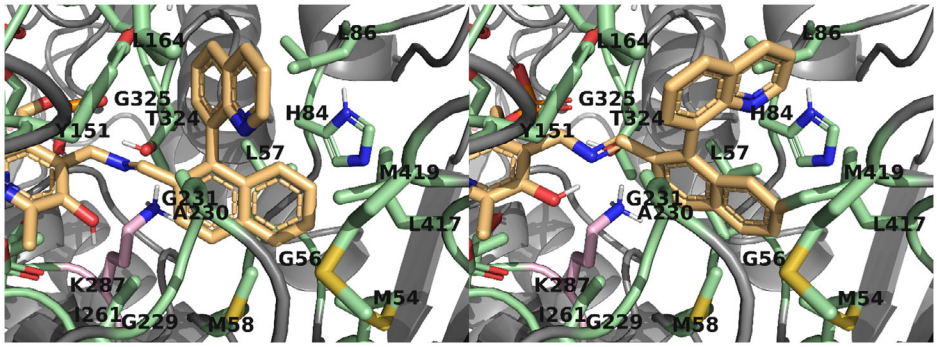

FIGURE 2 | Docking of (*S*)-**1i** (left) and (*R*)-**1i** (right) into the active site of *Pj*STA-R6-8, with docking scores of 3.68 and 0.1 kcal mol^{-1}, respectively. Compared to the (*S*)-enantiomer, the (*R*)-enantiomer is involved in a steric clash with L417 and the imine bond is positioned further from the catalytic K287 (pink). Noncatalytic residues within 4 Å of the docked quinonoid (beige) are shown in green. Dockings were performed in YASARA and visualized with PyMOL.

solubility. Additional polar solvents, including ethanol, DMF, acetonitrile, and 2-methyltetrahydrofuran (a renewable biobased solvent), were also evaluated (see Table S5). Among these, DMSO consistently afforded the highest conversions and/or optical purities for both transaminase-catalyzed reactions.

As for the naphthyl derivative, ATA-P1-G05 proved optimal for the transamination of the tolyl derivative **1n**, affording (*R*)-**2n** with 24% conversion and 96% *ee* (entry 1, Table 3). Other ATAs tested catalyzed the formation of the desired (*R*)- or (*S*)-amine from **1l** but generally exhibited lower conversions and optical purities around 50%. *Pj*STA-R6-8 was also able to catalyze the formation of atropisomeric amine (*S*)-**2n**, albeit with modest conversion and 73% *ee* (entry 7) after 24 h. Extending the reaction time to 96 h at 45°C improved conversion to 30%, while maintaining enantioselectivity (entry 10). In contrast, increasing the temperature negatively affects both activity and selectivity of ATA-P1-G05, yielding only 14% of (*R*)-**2l** with 85% *ee* after 96 h (entry 9).

The most suitable biocatalyzed transaminations for each of the starting materials **1a–n** were scaled up to the multimilligram scale (Table 4). Reactions were conducted using the corresponding heterobiaryl aldehydes (20 mM) for 48–72 h, followed by in situ acetylation of the resulting amines to afford the corresponding chiral amides (*S*)- or (*R*)-**3a–l**, with yields from 35% to 92% and optical purities between 52% and 99%.

Finally, computational studies at the DFT SMD(CH_2Cl_2)-BP98-D3BJ/def2-TZVP level of theory (see Supporting Information) were performed to estimate the racemization barriers of

TABLE 3 | DKR of heterobiaryl aldehyde (±)-**1n** employing ATAs. Substrate (5 mM) was dissolved in an ethanolamine buffer 0.1 M pH 7.5 with 10% v/v DMSO containing PLP (1.0 mM), $^{i}PrNH_2$ (1.0 M), and the corresponding ATA (10 mg).

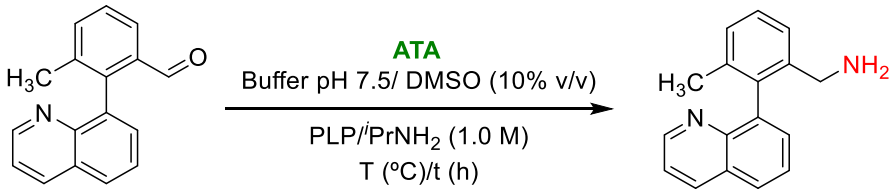

(±)-**1n** (*R*)- or (*S*)-**2n**

Entry	TA	*T*, ºC	*t*, h	[%]-2n[a]	*ee* (*S*)-2n, %[a]	Config.
1	ATA-P1-G05	30	24	24	96	*R*
2	ATA-013	30	24	22	56	*R*
3	ATA-025	30	24	21	53	*R*
4	ATA-217	30	24	26	54	*R*
5	ATA-234	30	24	26	51	*R*
6	ATA-237	30	24	24	28	*S*
7	*Pj*STA-R6-8	30	48	17	73	*S*
8	ATA-P1-G05	30	48	26	94	*R*
9	ATA-P1-G05	45	96	13	85	*R*
10	*Pj*STA-R6-8	45	96	30	75	*S*

[a]Measured by HPLC after acetylation of the resulting amine **2l**.

TABLE 4 | DKR of heterobiaryl aldehydes (±)-**1a–l** at multimilligram scale in the presence of TAs.

Entry	Aldehyde	TA	*t*, h	Isolated yield 3i–k, %[a]	*ee* 3i–k, %[b]	Config.
1	**1a**	ATA-013	48	89	97	*S*
2	**1b**	ATA-237	48	85	78	*S*
3	**1c**	ATA-303	72	35	63	*S*
4	**1c**	ATA-412	48	81	80	*R*
5	**1d**	ATA-013	48	65	94	*S*
6	**1e**	ATA-013	48	93	91	*S*
7	**1f**	ATA-237	48	86	52	*S*
8	**1g**	ATA-013	48	92	≥99	*S*
9	**1h**	ATA-P!-G05	48	90	96	*S*
10	**1i**	ATA-P1-G05	72	65	97	*R*
11	**1i**	*Pj*STA-R6-8	72	66	85	*S*
12	**1j**	ATA-234	72	40	73	*R*
13	**1k**	*Pj*STA-R6-8	72	25	≥99	*S*
14	**1l**	ATA-234	72	47	83	*R*
15	**1l**	*Pj*STA-R6-8	72	30	≥99	*S*
16	**1m**	ATA-234	48	80	79	*R*
17	**1n**	ATA-P1-G05	72	42	96	*R*

[a]Isolated yield after chromatographic purification.
[b]Determined by HPLC after acetylation.

2-(quinoline-8-yl) naphthaldehyde (**1i**) and its corresponding amine derivative **2i**. For compound **1i**, a racemization barrier of 21.1 kcal mol^{-1} was calculated, with a transition state featuring the key N···CHO interaction. When the corresponding imine derivative formed in the transamination is considered, the barrier increases to 24.7 kcal mol^{-1}. Nevertheless, both barriers are consistent with racemization taking place at rates compatible with DKR under the experimental conditions. In sharp contrast, a significantly higher barrier of 30.5 kcal mol^{-1} was calculated for the amine **2i**, conferring high configurational stability, with anestimated half-life of 80.6 years at 25°C (the half-life has been estimated from the calculated racemization barrier using the Eyring equation, $\kappa = \frac{k_B T}{h} e^{-\Delta G^{\ddagger}/RT}$, assuming first-order kinetics: $t_{1/2} = \frac{ln2}{\kappa}$). Furthermore, the rotational barrier around the C–N stereogenic axis in the *N*-arylindole diamine **2a** was also computed. Unlike the aldehyde substrate **1a** (calculated barrier 18.6 kcal mol^{-1}) [51], amine **2a** lacks the LABI system, and the calculated barrier of 27.8 kcal mol^{-1} for the corresponding transition state for atropisomerization is, as expected, substantially higher, further supporting the configurational stability of the products. The racemization barriers for amines **2a** and **2i** were determined experimentally (see Supporting Information), giving values of 28.0 Kcal mol^{-1} for **2a** and 31.7 Kcal mol^{-1} for **2i**, which are in good agreement with those obtained from computational studies.

3 | Conclusion

An efficient biocatalytic DKR strategy for the atroposelective synthesis of heterobiaryl amines has been developed, including *N*-arylindole diamines and 2-(quinolin-8-yl)benzyl amines. This novel approach exploits the transient formation of Lewis acid–base pairs between the heterocyclic/NMe_2 nitrogen and the in situ generated imino group, facilitating substrate racemization via a six-membered cyclic transition states. Subsequent atroposelective reductive amination, catalyzed by transaminases, enabled the synthesis of a broad array of atropisomeric heterobiaryl indole diamines and quinoline-based amines with moderate to high yields and enantioselectivities. The resulting axially chiral products represent valuable scaffolds with significant potential as ligands in asymmetric catalysis.

Author Contributions

Juan M. Coto-Cid: investigation (equal), original writing (support). **Patricia Rodríguez-Salamanca:** investigation (equal). **Christian M. Heckmann:** investigation, methodology. **Caroline E. Paul:** funding adquisition, review & editing. **Joaquín López-Serrano:** methodology, review & editing. **Rosario Fernández:** funding adquisition, review & editing. **José M. Lassaletta:** funding adquisition, formal analysis, review & editing. **Valentín Hornillos:** conceptualization, review & editing. **Gonzalo de Gonzalo:** conceptualization (lead), original writing (lead).

Acknowledgments

J.L.-S. acknowledges the use of computational facilities of the Centro Informático Científico de Andalucía (CICA, cluster Hercules). This work is dedicated to the memoryof Professor Iván Lavandera.

Funding

The work was supported by Spanish Ministerio de Ciencia e Innovación (Grant PID2022-143230NB-I00), European funding (ERDF), and Junta de Andalucía (Grant P18-FR-3531). C.M.H.: This project has received funding from the European Union (MSCA, Grant Agreement No. 101062327).

Views and opinions expressed are however those of the authors only and do not necessarily reflect those of the European Union or European Research Council. Neither the European Union nor the granting authority can be held responsible for them. C.E.P.: This project has received funding from the European Research Council (ERC) under the European Union's Horizon 2020 research and innovation programme (Grant No. 949910).

Conflicts of Interest

The authors declare no conflicts of interest.

Data Availability Statement

The data that supports the findings of this study are available in the Supporting Information of this article.

References

1. P. W. Glunz, "Recent Encounters with Atropisomerism in Drug Discovery," *Bioorganic & Medicinal Chemistry Letters* 28 (2018): 53–60.

2. M. Basilaia, M.-H. Chen, J. Secka, and J. L. Gustafson, "Atropisomerism in the Pharmaceutically Relevant Realm," *Accounts of Chemical Research* 55 (2022): 2904–2919.

3. G. Bringmann, T. Gulder, T. A. M. Gulder, and M. Breuning, "Atroposelective Total Synthesis of Axially Chiral Biaryl Natural Products," *Chemical Reviews* 111 (2011): 563–639.

4. J. Clayden, W. J. Moran, P. J. Edwards, and S. R. LaPlante, "The Challenge of Atropisomerism in Drug Discovery," *Angewandte Chemie International Edition* 48 (2009): 6398–6401.

5. For a comprehensive book review, see: Q.-L. Zhou, ed., *Privileged Chiral Ligands and Catalysts* (Wiley-VCH, 2011).

6. B. Tan, ed., *Axially Chiral Compounds: Asymmetric Synthesis and Applications* (Wiley-VCH, 2021).

7. For selected reviews, see: W. Tang and X. Zhang, "New Chiral Phosphorus Ligands for Enantioselective Hydrogenation," *Chemical Reviews* 103 (2003): 3029–3070.

8. T. Akiyama, "Stronger Brønsted Acids," *Chemical Reviews* 107 (2007): 5744–5758.

9. Y.-M. Li, F.-Y. Kwong, W.-Y. Yu, and A. S. C. Chan, "Recent Advances in Developing New Axially Chiral Phosphine Ligands for Asymmetric Catalysis," *Coordination Chemistry Reviews* 251 (2007): 2119–2144.

10. J.-H. Xie and Q.-L. Zhou, "Chiral Diphosphine and Monodentate Phosphorus Ligands on a Spiro Scaffold for Transition-Metal-Catalyzed Asymmetric Reactions," *Accounts of Chemical Research* 41 (2008): 581–593.

11. D. Parmar, E. Sugiono, S. Raja, and M. Rueping, "Complete Field Guide to Asymmetric Binol-Phosphate Derived Brønsted Acid and Metal Catalysis: History and Classification by Mode of Activation; Brønsted Acidity, Hydrogen Bonding, Ion Pairing, and Metal Phosphates," *Chemical Reviews* 114 (2014): 9047–9153.

12. M. P. Carroll and P. J. Guiry, "P, N Ligands in Asymmetric Catalysis," *Chemical Society Reviews* 43 (2014): 819–833.

13. G. Dotsevi, Y. Sogah, and D. J. Cram, "Total Chromatographic Optical Resolutions of α-Amino Acid and Ester Salts through Chiral Recognition by a Host Covalently Bound to Polystyrene Resin," *Journal of the American Chemical Society* 98 (1976): 3038–3041.

14. K. Takaishi, M. Yasui, and T. Ema, "Binaphthyl–bipyridyl Cyclic Dyads as a Chiroptical Switch," *Journal of the American Chemical Society* 140 (2018): 5334–5338.

15. Q. Li, L. Green, N. Venkataraman, I. Shiyanovskaya, and A. Khan, "Reversible Photoswitchable Axially Chiral Dopants with High Helical Twisting Power," *Journal of the American Chemical Society* 129 (2007): 12908–12909.

16. M. Mccormick, J. Mcguire, G. Pittenger, R. Pittenger, and W. M. Stark, "Vancomycin, a New Antibiotic. I. Chemical and Biologic Properties," *Antibiotics Annual* 3 (1955): 606–611.

17. Q. Shi, K. Chen, X. Chen, et al., "Antitumor Agents. 183. Syntheses, Conformational Analyses, and Antitubulin Activity of Allothiocolchicinoids," *The Journal of Organic Chemistry* 63 (1998): 4018–4025.

18. D. Uraguchi, K. Koshimoto, S. Miyake, and T. Ooi, "Chiral Ammonium Betaines as Ionic Nucleophilic Catalysts," *Angewandte Chemie International Edition* 49 (2010): 5567–5569.

19. T. Kano, R. Sakamoto, M. Akakura, and K. Maruoka, "Stereocontrolled Synthesis of Vicinal Diamines by Organocatalytic Asymmetric Mannich Reaction of N-Protected Aminoacetaldehydes: Formal Synthesis of (−)-Agelastatin A," *Journal of the American Chemical Society* 134 (2012): 7516–7520.

20. J. A. Carmona, C. Rodríguez-Franco, J. López-Serrano, et al., "Atroposelective Transfer Hydrogenation of Biaryl Aminals via Dynamic Kinetic Resolution. Synthesis of Axially Chiral Diamines," *ACS Catalysis* 11 (2021): 4117–4124.

21. M. Furegati and A. J. Rippert, "An Approach to New, Axially Chiral ζ-Amino Alcohols Using a ring Opening Reaction," *Synlett* 7 (2002): 1158–1160.

22. D. Uraguchi, K. Koshimoto, and T. Ooi, "Flexible Synthesis, Structural Determination, and Synthetic Application of a New C 1-Symmetric Chiral Ammonium Betaine," *Chemical Communications* 46 (2010): 300–302.

23. X. Zhang, X. Xue, and Z. Gu, "Stereoselective Synthesis Axially Chiral Arylnitriles through Base-Induced Chirality-Relay β-Carbon Elimination of α-Hydroxyl Ketoxime Esters," *Organic Letters* 25 (2023): 3602–3606.

24. J. A. Carmona, C. Rodríguez-Franco, R. Fernández, V. Hornillos, and J. M. Lassaletta, "Atroposelective Transformation of Axially Chiral (hetero)biaryls. From Desymmetrization to Modern Resolution Strategies," *Chemical Society Reviews* 50 (2021): 2968–2983.

25. J. K. Cheng, S. H. Xiang, S. Li, L. Ye, and B. Tan, "Recent Advances in Catalytic Asymmetric Construction of Atropisomers," *Chemical Reviews* 121 (2021): 4805–4902.

26. Q. Zhao, C. Peng, Y.-T. Wang, G. Zhan, and B. Han, "Recent Progress on the Construction of Axial Chirality through Transition-Metal-Catalyzed Benzannulation," *Organic Chemistry Frontiers* 8 (2021): 2772–2785.

27. C.-X. Liu, W.-W. Zhang, S.-Y. Yin, Q. Gu, and S.-L. You, "Synthesis of Atropisomers by Transition-Metal-Catalyzed Asymmetric C–H Functionalization Reactions," *Journal of the American Chemical Society* 143 (2021): 14025–14040.

28. P. Rodríguez-Salamanca, R. Fernández, V. Hornillos, and J. M. Lassaletta, "Asymmetric Synthesis of Axially Chiral C-N Atropisomers," *Chemistry: A European Journal* 28 (2022): e202104442.

29. C. B. Roos, C. H. Chiang, L. A. M. Murray, D. Yang, L. Schulert, and A. R. H. Narayan, "Stereodynamic Strategies to Induce and Enrich Chirality of Atropisomers at a Late Stage," *Chemical Reviews* 123 (2023): 10641–10727.

30. K. Mori, T. Itakura, and T. Akiyama, "Enantiodivergent Atroposelective Synthesis of Chiral Biaryls by Asymmetric Transfer Hydrogenation: Chiral Phosphoric Acid Catalyzed Dynamic Kinetic Resolution," *Angewandte Chemie International Edition* 55 (2016): 11642–11646.

31. J. Zhang and J. Wang, "Atropoenantioselective Redox-Neutral Amination of Biaryl Compounds through Borrowing Hydrogen and Dynamic Kinetic Resolution," *Angewandte Chemie International Edition* 57 (2017): 465–469.

32. A. Kim, J. Moon, C. Lee, J. Song, J. Kim, and Y. Kwon, "Organocatalytic Atroposelective Synthesis of Isoquinolines via Dynamic Kinetic Resolution," *Organic Letters* 24 (2022): 1077–1082.

33. E. L. Bell, W. Finnigan, S. P. France et al.," Biocatalysis," *Nature Reviews Methods Primers* 1 (2021): 46.

34. S. Wu, R. Snajdrova, J. C. Moore, K. Baldenius, and U. T. Bornscheuer, "Biocatalysis: Enzymatic Synthesis for Industrial Applications," *Angewandte Chemie International Edition* 60 (2021): 88–119.

35. M. Hall, Biocatalysis for Practitioners, ed. G. de Gonzalo, and I. Lavandera (Wiley-VCH, 2021), 181–223.

36. N. Aoyagi and T. Izumi, "Kinetic Resolution of 1,1′-Binaphthylamines via Lipase-Catalyzed Amidation," *Tetrahedron Letters* 43 (2002): 5529–5531.

37. P. Zhang, B. Yuan, J. Li, et al., "Biocatalytic Desymmetrization for the Atroposelective Synthesis of Axially Chiral Biaryls Using an Engineered Imine Reductase," *Angewandte Chemie International Edition* 64 (2024): e202416569.

38. W.-Q. Zheng, X.-X. Zhu, Z. Zhu, et al., "Access to Axially Chiral Biaryl Benzylamines via Ancestral Enzyme-Enabled Reductive Amination Desymmetrization," *ACS Catalysis* 15 (2025): 1522–1531.

39. X. Hao, Z. Tian, Z. Yao, et al., "Atroposelective Synthesis of Axial Biaryls by Dynamic Kinetic Resolution Using Engineered Imine Reductases," *Angewandte Chemie International Edition* 63 (2024): e202410112.

40. X. Hao, B. Wang, Z. Tian, et al., "Biocatalytic Atroposelective Synthesis of Heterobiaryls and Heterobiaryl *N*-Oxides via Dynamic Kinetic Resolution," *Organic Chemistry Frontiers* 12 (2025): 2658–2669.

41. E. Cananà, F. Rinaldi, and M. L. Contente, "Biocatalysis in Non-Conventional Media: Unlocking the Potential for Sustainable Chiral Amine Synthesis," *Chemistry: A European Journal* 30 (2024): e202304364.

42. S. A. Kelly, S. Mix, T. S. Moody, and B. F. Gilmore, "Transaminases for Industrial Biocatalysis: Novel Enzyme Discovery," *Applied Microbiology and Biotechnology* 104 (2020): 4781–4794.

43. B. N. Hogg, C. Schnepel, J. D. Finnigan, S. J. Charnock, M. A. Hayes, and N. J. Turner, "The Impact of Metagenomics on Biocatalysis," *Angewandte Chemie International Edition* 63 (2024): e202402316.

44. M. S. Madsen and J. M. Woodley, "Considerations for the Scale-up of In Vitro Transaminase-Catalyzed Asymmetric Synthesis of Chiral Amines," *ChemCatChem* 15 (2023): e202300560.

45. F. Falcioni, L. Humphreys, R. C. Lloyd et al., "The Evolving Landscape of Industrial Biocatalysis in Perspective from the ACS Green Chemistry Institute Pharmaceutical Roundtable," *ACS Catalysis* 17 (2025): 10780–10794.

46. V. Hornillos, J. A. Carmona, A. Ros, et al., "Dynamic Kinetic Resolution of Heterobiaryl Ketones by Zinc-Catalyzed Asymmetric Hydrosilylation," *Angewandte Chemie International Edition* 57 (2018): 3777–3781.

47. J. A. Carmona, P. Rodríguez-Salamanca, R. Fernández, J. M. Lassaletta, and V. Hornillos, "Dynamic Kinetic Resolution of 2-(quinolin-8-Yl)benzaldehydes: Atroposelective Iridium-Catalyzed Transfer Hydrogenative Allylation," *Angewandte Chemie International Edition* 62 (2023): e202306981.

48. C. Rodríguez-Franco, A. Ros, P. Merino, R. Fernández, J. M. Lassaletta, and V. Hornillos, "Dynamic Kinetic Resolution of Indole-Based Sulfenylated Heterobiaryls by Rhodium-Catalyzed Atroposelective Reductive Aldol Reaction," *ACS Catalysis* 13 (2023): 12134–12141.

49. C. Rodríguez-Franco, E. Roldán-Molina, A. Aguirre-Medina, R. Fernández, V. Hornillos, and J. M. Lassaletta, "Catalytic Atroposelective Synthesis of C-N Axially Chiral Aminophosphines via Dynamic Kinetic Resolution," *Angewandte Chemie International Edition* 63 (2024): e202409524.

50. For a Recent Review See: J. A. Carmona, C. Rodríguez-Franco, R. Fernández, J. M. Lassaletta, and V. Hornillos, "Lewis Acid-Base Interactions as a Racemization Strategy for the Atroposelective Synthesis of (hetero)biaryls via Dynamic Kinetic Resolution," *ChemCatChem* 16 (2024): e202400701,

51. P. Rodríguez-Salamanca, G. de Gonzalo, J. A. Carmona et al., "Biocatalytic Atroposelective Synthesis of Axially Chiral *N*-Arylindoles via Dynamic Kinetic Resolution," *ACS Catalysis* 13 (2023): 659–664.

52. J. M. Coto-Cid, G. de Gonzalo, J. A. Carmona et al., "Atroposelective Synthesis of 2-(quinolin-8-Yl)benzyl Alcohols by Biocatalytic Dynamic Kinetic Resolutions," *Advanced Synthesis & Catalysis* 366 (2024): 909–915.

53. J. M. Coto-Cid, V. Hornillos, R. Fernández, J. M. Lassaletta, and G. de Gonzalo, "Chemoenzymatic Dynamic Kinetic Resolution of Atropisomeric 2-(quinolin-8-Yl)benzylalcohols," *The Journal of Organic Chemistry* 90 (2025): 5120–5124.

54. Q. Meng, C. Ramírez-Palacios, N. Capra, et al., "Computational Redesign of an ω-Transaminase from *Pseudomonas Jessenii* for Asymmetric Synthesis of Enantiopure Bulky Amines," *ACS Catalysis* 11 (2021): 10733–10747.

55. C. M. Heckmann and C. E. Paul, "Enantio-Complementary Synthesis of 2-Substituted Pyrrolidines and Piperidines via Transaminase-Triggered Cyclizations," *JACS Au* 3 (2023): 1642–1649.

Supporting Information

Additional supporting information can be found online in the Supporting Information section. **Supporting Fig. S1a:** Calculated energy profile for the rotation around the C—C axis of aldehyde **1i**. Data are relative free energies in kcal·mol^{-1}. **Supporting Fig. S1b:** Calculated energy profile for the rotation around the C—C axis of the imine derivative from the condensation of the aldehyde **1i** and ammonia. Data are relative free energies in kcal·mol^{-1}. **Supporting Fig. S2:** Calculated energy profile for the rotation around the C—C axis of heterobiaryl amine **2i**. Data are relative free energies in kcal·mol^{-1}. **Supporting Fig. S3:** Laplacian,$\nabla^2\rho$, of the electron density of **intX** on the quinoline plane superimposed on its calculated molecular structure, showing bond critical points (bcp) of the electron density, ρ, as blue dots. The quinoline N—CHO bond distance is shown in angstrom. The text box summarizes relevant values of the N—CHO bcp. Dashed-blue trace and solid-red trace are for negative and positive values of $\nabla^2\rho$, respectively. **Supporting Fig. S4:** Calculated energy profile for the rotation around the C—C axis of **2a**. Data are relative free energies in kcal·mol^{-1}. **Supporting Table S1:** Biocatalyzed transamination of heterobiaryl aldehyde (±)-**1a**. **Supporting Table S2:** Effect of heterobiaryl aldehyde **1a** concentration in the biocatalyzed transamination in presence of ATA-013. **Supporting Table S3:** Biocatalyzed transamination of heterobiaryl aldehydes (±)-**1b-h**. **Supporting Table S4:** Biocatalyzed transamination of heterobiaryl aldehydes (±)-**1i-m**. **Supporting Table S5:** Solvent effect in the synthesis of heterobiaryl amine **2i**. **Supporting Table S6:** Biocatalyzed transamination of heterobiaryl aldehyde (±)-**1n**. **Supporting Table S7:** GC retention times for the determination of conversion.